

****FULL TITLE****

*ASP Conference Series, Vol. **VOLUME**, **YEAR OF PUBLICATION***

****NAMES OF EDITORS****

The origin and physical mechanism of the ensemble Baldwin effect

Xiaobo Dong¹, Jianguo Wang^{2,1}, Tinggui Wang¹, Huiyuan Wang¹,
Xiaohui Fan³, Hongyan Zhou¹, Weimin Yuan², and Qian Long⁴

Abstract. We have conducted a systematic investigation of the origin and underlying physics of the line–line and line–continuum correlations of AGNs, particularly the Baldwin effect. Based on the homogeneous sample of Seyfert 1s and QSOs in the SDSS DR4, we find the origin of all the emission-line regularities is Eddington ratio (L/L_{Edd}). The essential physics is that L/L_{Edd} regulates the distributions of the properties (particularly column density) of the clouds bound in the line-emitting region.

1. Baldwin effect and its three 2nd-order effects

Active galactic nuclei (AGNs; including QSOs) are essentially a kind of radiation and line-emitting systems powered by gravitational accretion onto supermassive black holes. The global spectra of AGNs are remarkably similar, emission lines with similar intensity ratios sitting atop a blue continuum that has a similar slope among AGNs regardless of their luminosities and redshifts (Davidson & Netzer 1979, Korista 1999). However, this similarity is only a zeroth-order approximation; in 1977, Baldwin found that, among the QSO ensemble, the equivalent width (EW) of the CIV $\lambda 1549$ emission line correlates negatively with the continuum luminosity (Baldwin 1977). From then on, such a negative EW–L correlation has been found for almost all emission lines in the ultraviolet and optical bands, and has been termed as “Baldwin effect” (hereafter BEff; see Osmer & Shields 1999, Shields 2007 for reviews).¹ Furthermore, also found are the three kinds of 2nd-order effects of the BEff, namely, the dependence of the BEff slope (the slope of the log EW–log L relation) on luminosity, on ionization energy, and, particularly, on velocity. The CIV BEff is stronger in the peak and red wing than in the blue (Francis & Koratkar 1995, Richards et al. 2002)! The

¹Center for Astrophysics, University of Science and Technology of China, Hefei, Anhui 230026, China; xbdong@ustc.edu.cn

²National Astronomical Observatories/Yunnan Observatory, Chinese Academy of Sciences, P.O. Box 110, Kunming, Yunnan 650011, China

³Steward Observatory, The University of Arizona, Tucson, AZ 85721

⁴Department of Precision Machinery and Instrumentation, University of Science and Technology of China, Hefei, Anhui 230026, China

¹To distinguish the BEff in the ensemble from a similar correlation present in individual variable AGNs, the former is usually called “the ensemble BEff” that is the topic of this paper.

velocity dependence betrays the nature of the BEff: this kind of negative correlation relates to the line-emitting gas gravitationally bound in the broad-line region (BLR).

2. The origin and the physical mechanism

In order to explore the origin and the underlying mechanism of the BEff, based on the homogeneous sample of 4178 $z \leq 0.8$ Seyfert 1s and QSOs with median spectral S/N $\gtrsim 10$ per pixel in the SDSS DR4, we have conducted a systematic investigation of the line–line and line–continuum correlations for broad and narrow emission lines in the near-UV and optical, from Mg II $\lambda 2800$ to [O III] $\lambda 5007$. Our findings are as follows:

(i) The strongest correlations of almost all the emission-line intensity ratios and EWs are with L/L_{Edd} , either positively (e.g. Fe II EW) or negatively (e.g. Mg II EW), rather than with L or M_{BH} ; besides, generally intensity ratios have tighter correlations with L/L_{Edd} than the EWs of the related lines.

(ii) The intensity ratios of Fe II emissions – both narrow and broad – to Mg II have very strong, positive correlations with L/L_{Edd} ; interestingly enough, (narrow Fe II $\lambda 4570$)/Mg II has a stronger correlation with L/L_{Edd} than the optical and UV (broad Fe II)/Mg II, with Spearman $r_s = 0.74$ versus 0.58 (optical) and 0.46 (UV); see Fig. 1 (Dong et al. 2009a).

These findings argue that Eddington ratio ($\ell \equiv L/L_{\text{Edd}}$)² is the origin of the BEff, as of other regularities of almost all emission lines (e.g., the Fe II–[O III] anticorrelation, Boroson & Green 1992). This once has been suggested by Baskin & Laor (2004) and Bachev et al. (2004) for the C IV BEff. We propose that the underlying physics is certain self-regulation mechanisms caused by (or corresponding to) L/L_{Edd} ; these mechanisms maintain the normal dynamically quasi-steady states of the gas surrounding the central engine of AGNs (Dong et al. 2009a,b). Briefly, the essential one is that *there is a lower limit on the column density (N_{H}) of the clouds gravitationally bound in the AGN line-emitting region, set by L/L_{Edd}* (hereafter the $N_{\text{H}}-L/L_{\text{Edd}}$ mechanism; see also Fig. 1 of Fabian et al. 2006, Marconi et al. 2008). As L/L_{Edd} increases, the emission strength decreases for high-ionization lines (e.g. C IV) and optically thick lines that are emitted at the illuminated surface (e.g. Ly α) or in the thin transition layer (e.g. Mg II) of the BLR clouds; for low-ionization, optically thin lines such as

² Eddington ratio is the ratio between the bolometric and Eddington luminosities. Eddington luminosity (L_{Edd}), by definition, is the luminosity at which the gravity of the central source acting on an electron–proton pair (i.e. fully ionized gas) is balanced by the radiation pressure due to electron Thomson scattering; $L_{\text{Edd}} = 4\pi GcMm_{\text{p}}/\sigma_{\text{T}}$, where G , c , M , m_{p} , σ_{T} are the gravitational constant, speed of light, mass of the central source, proton mass, Thomson scattering cross-section, respectively. In accretion-powered radiation systems, L/L_{Edd} is often referred to as *dimensionless accretion rate* \dot{m} (the relative accretion rate normalized by Eddington accretion rate \dot{M}_{Edd} , $\dot{m} \equiv \dot{M}/\dot{M}_{\text{Edd}} = \eta c^2 \dot{M}/L_{\text{Edd}}$, \dot{M} being mass accretion rate and η the accretion efficiency) as \dot{m} is not an observable; yet the two notations are different both in meaning and in scope of application. Even in the accretion-powered radiation systems like AGNs, L/L_{Edd} (L) is not equivalent to \dot{m} (\dot{M}) except in the simple thin accretion disk model of Shakura & Sunyaev (1973). Therefore, we would rather call L/L_{Edd} *dimensionless luminosity* (ℓ).

Fe II multiplets that originate from the volume behind the Hydrogen ionization front (i.e., from the ionization-bounded clouds only), as L/L_{Edd} increases the emission strength increases.³ This is schematically sketched in Fig. 2.

3. The implications

I. An implication is that BG92’s PC1, if only the spectral correlations in the UV–optical are concerned, shares the same origin with PC2 that is exactly the He II BEff. A lesson is that we should be more cautious about the premises of blind source separation methods such as Principal Component Analysis.

II. As suggested insightfully by G. Richards (e.g. Richards 2006), *the CIV line blueshifting (in other words, blue asymmetry) is the same phenomenon of BEff.* The underlying physical picture is clear now: There are two components in the CIV emission, one arising from outflows and the other from the clouds gravitationally bound in the BLR; the fraction of bound clouds that optimally emit CIV line decreases with increasing L/L_{Edd} according to the $N_{\text{H}} - L/L_{\text{Edd}}$ mechanism.

III. If the observed large scatter of Fe II/Mg II at the same redshift is caused predominately by the diversity of L/L_{Edd} , then once this systematic variation is corrected according to the tight Fe II/Mg II – L/L_{Edd} correlation, it is hopeful to still use Fe II/Mg II as a measure of the Fe/Mg abundance ratio and thus a cosmic clock (*at least in a statistical manner*).

Appendix: Not *Baldwin Effect*, but *ell Effect*?

This Appendix is to present more results taken from Dong et al. (2009b) that did not appear in the proceedings paper due to page limit. The aim is to show that the traditional BEff – the dependence of emission-line EWs on luminosity – is likely not to be fundamental, but derived from the dependence on Eddington ratio (ℓ). To avoid any confusion, below we call the latter ell effect (*ell* stands for ℓ , Eddington ratio).

The ell effect is the 1st-order small variation to the 0th-order global similarity of QSO spectra that is well explained by “locally optically-emitting clouds” (LOC) photoionization modeling (Baldwin et al. 1995). As discussed above, in the study of the QSO emission-line correlations, the focus seems to be shifting from the physics (*microphysics*) mainly of the accretion process to the ‘statistical physics’ (*macrophysics*) of the surrounding clouds (Korista 1999; Korista, private communication). With more realistic constraints to be accounted for [e.g., the distribution function of the cloud number with ℓ and N_{H} , $N_{\text{c}}(\ell, N_{\text{H}}(\ell))$]; cf.

³ Certainly, for particular radiation systems that are powered by gravitational accretion (e.g. AGNs), ℓ is linked tightly to \dot{m} anyway (cf. Footnote 2; Merloni & Heinz 2008). Thus there is an additional effect associated with ℓ yet directly via \dot{m} as follows. The increase in ℓ means, meanwhile, the increase in \dot{m} , the gas supply. Reasonably, it is from the supplied gas spiraling into the central engine that (at least a significant part of) the line-emitting clouds originate; this is particularly true for the BLR and inner NLR clouds that are located between the torus (as the fuel reservoir) and the accretion disk (e.g. Gaskell & Goosman 2008). Hence, as ℓ increases, the total mass of line-emitting gas increases.

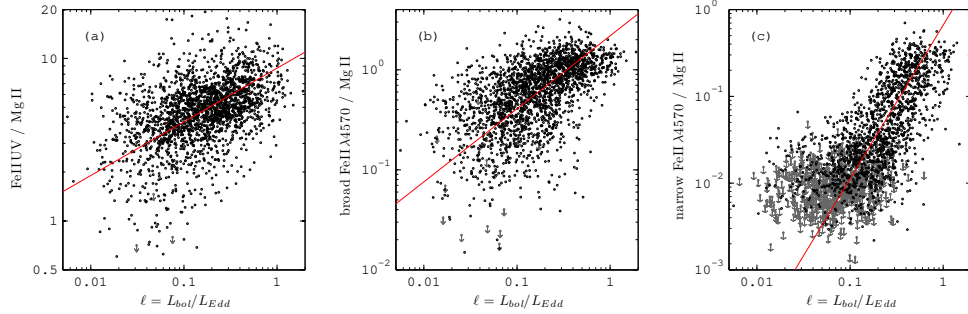


Figure 1. Plots of the intensity ratios of the broad and narrow Fe II emissions to Mg II $\lambda 2800$ versus Eddington ratio for the homogeneous sample of 4178 Seyfert 1s and QSOs. Also plotted are the best-fitted linear relations in the log–log scale (Dong et al. 2009a).

Fig. 2], the 1st-order regularities and even the 2nd-order effects of QSO emission lines (see §1) may be reproduced exactly by future LOC modeling.

Fig. 3 confirms that ℓ is the primary driver of the BEff of Mg II $\lambda 2800$. Fig. 4 shows that, at the 0th-order approximation, Mg II luminosity is directly proportional to the continuum luminosity, exactly as predicted by photoionization theory; at the 1th-order approximation, for different ℓ the proportional coefficient is different, $\log k \simeq \log k_0 + k' \cdot \log \ell$ — this is just the ell effect illustrated in Fig. 3c.

Some researchers once have found that the slopes of the emission line versus continuum luminosity relations in the log–log scale is not unity (see references in §2 of Shields 2007). We must note that this is likely not to be intrinsic (see Dong et al. 2009b for a detailed investigation). It is caused partly by selection effect inherent in any magnitude-limited sample, with high-luminosity objects having higher ℓ and thus smaller EWs. For optical emission lines particularly (e.g. H β), this is mainly caused by the contamination of the host-galaxy starlight (cf. Croom et al. 2002). The starlight contamination aggravates gradually towards longer wavelengths; moreover, within a fixed aperture, it aggravates with decreasing AGN luminosity.

In one word, a sole fundamental parameter, ℓ , well regulates the ordinary state of the surrounding gas that is inevitably inhomogeneous and clumpy (‘clouds’).

Acknowledgments. DXB thanks Kirk Korista, Martin Gaskell, Aaron Barth, Alessandro Marconi, Philippe Véron, Daniel Proga and Xueguang Zhang for the helpful discussions and comments, thanks Zhen-Ya Zheng for the help in improving IDL figures, and thanks Sheng-Miao Wu, Lei Chen and Fu-Guo Xie for their warm hospitality and brainstorming discussions during my visits in Shanghai Observatory. This work has made use of the data of the Sloan Digital Sky Survey (SDSS). The SDSS Web Site is <http://www.sdss.org/>. This work is supported by Chinese NSF grants NSF-10533050, NSF-10703006 and NSF-10728307, the CAS Knowledge Innovation Program (Grant No. KJCX2-YW-T05), and a National 973 Project of China (2007CB815403).

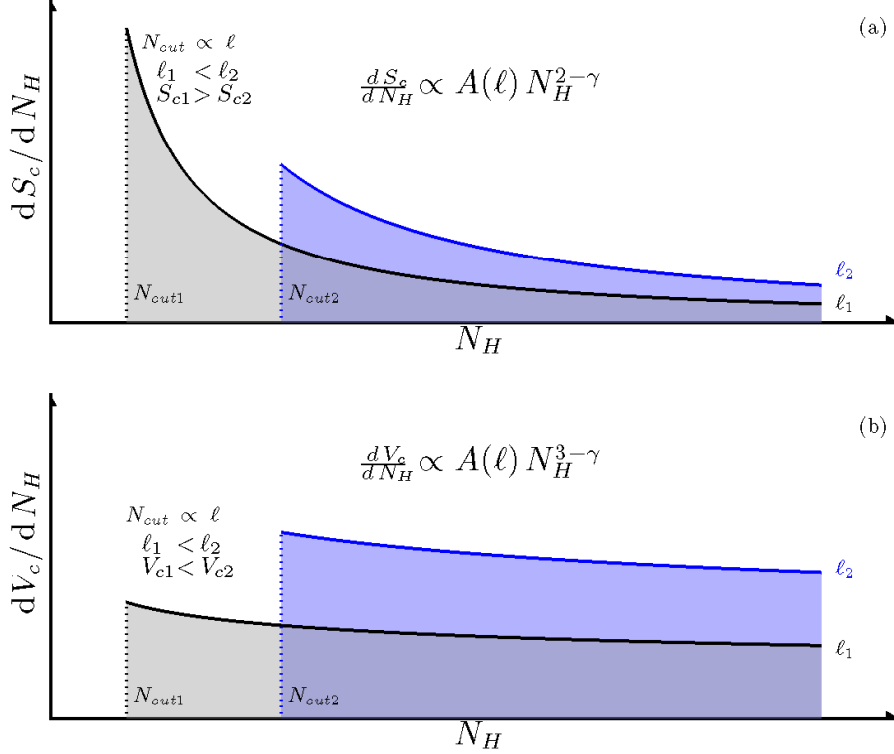


Figure 2. Schematic sketches of the distribution functions of the total illuminated surface area S_c with N_H (panel a) and of the total volume V_c with N_H (panel b) of the clouds bound in the broad-line region and inner narrow-line region of AGNs. The sketches are plotted assuming the distribution of the cloud number to be $dN_c/dN_H = A(\ell) N_H^{-\gamma}$ with $\gamma = 3.2$; the lower-limit N_H cutoff is set by the N_H-L/L_{Edd} mechanism, roughly scaling with L/L_{Edd} . Note that the strengths of high-ionization lines (e.g. CIV) and optically-thick lines (e.g. Ly α and MgII) are roughly proportional to S_c while that of low-ionization, optically-thin lines such as narrow-line and broad-line FeII roughly proportional to V_c (Dong et al. 2009b).

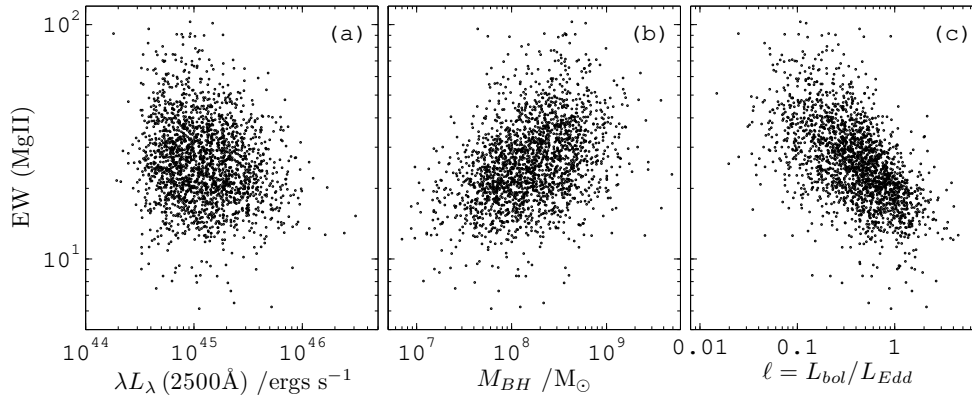


Figure 3. The relation between the equivalent width of Mg II $\lambda 2800$ of the 2092 type-1 AGNs in the $z > 0.45$ subsample and their $\lambda L_{\lambda}(2500\text{\AA})$, black hole mass (M_{BH}), and Eddington ratio ($\ell \equiv L_{\text{bol}}/L_{\text{Edd}}$).

References

- Bachev, R., et al. 2004, ApJ, 617, 171
 Baldwin, J. A. 1977, ApJ, 214, 679
 Baldwin, J., Ferland, G., Korista, K., & Verner, D. 1995, ApJ, 455, L119
 Baskin, A., & Laor, A. 2004, MNRAS, 350, L31
 Boroson, T. A. & Green, R. F. 1992, ApJS, 80, 109 (BG92)
 Croom, S. M., et al. 2002, MNRAS, 337, 275
 Davidson, K., & Netzer, H. 1979, Reviews of Modern Physics, 51, 715
 Dong, X., Wang, J., Wang, T., Wang, H., Fan, X., Zhou, H., Yuan, W. 2009a, arXiv:0903.5020
 Dong, X., Wang, J., Wang, T., Wang, H., Fan, X., Zhou, H., Yuan, W., Qian, L. 2009b, ApJ to be submitted
 Fabian, A. C., Celotti, A., & Erlund, M. C. 2006, MNRAS, 373, L16
 Francis, P. J., & Koratkar, A. 1995, MNRAS, 274, 504
 Gaskell, C. M., & Goosmann, R. W. 2008, arXiv:0805.4258
 Korista, K. 1999, Quasars and Cosmology, ASPC, 162, 429
 Marconi, A., Axon, D. J., Maiolino, R., Nagao, T., Pastorini, G., Pietrini, P., Robinson, A., & Torricelli, G. 2008, ApJ, 678, 693
 Merloni, A., & Heinz, S. 2008, MNRAS, 388, 1011
 Osmer, P. S., & Shields, J. C. 1999, Quasars and Cosmology, ASPC, 162, 235
 Richards, G. T., Vanden Berk, D. E., Reichard, T. A., Hall, P. B., Schneider, D. P., SubbaRao, M., Thakar, A. R., & York, D. G. 2002, AJ, 124, 1
 Richards, G. T. 2006, arXiv:astro-ph/0603827 (talk presented at the ‘‘AGN Winds in the Caribbean’’ Workshop, St. John, USVI; 28 November - 2 December, 2005; <http://www.nhn.ou.edu/~leighly/VImeeting/>)
 Shields, J. C. 2007, The Central Engine of Active Galactic Nuclei, ASPC, 373, 355

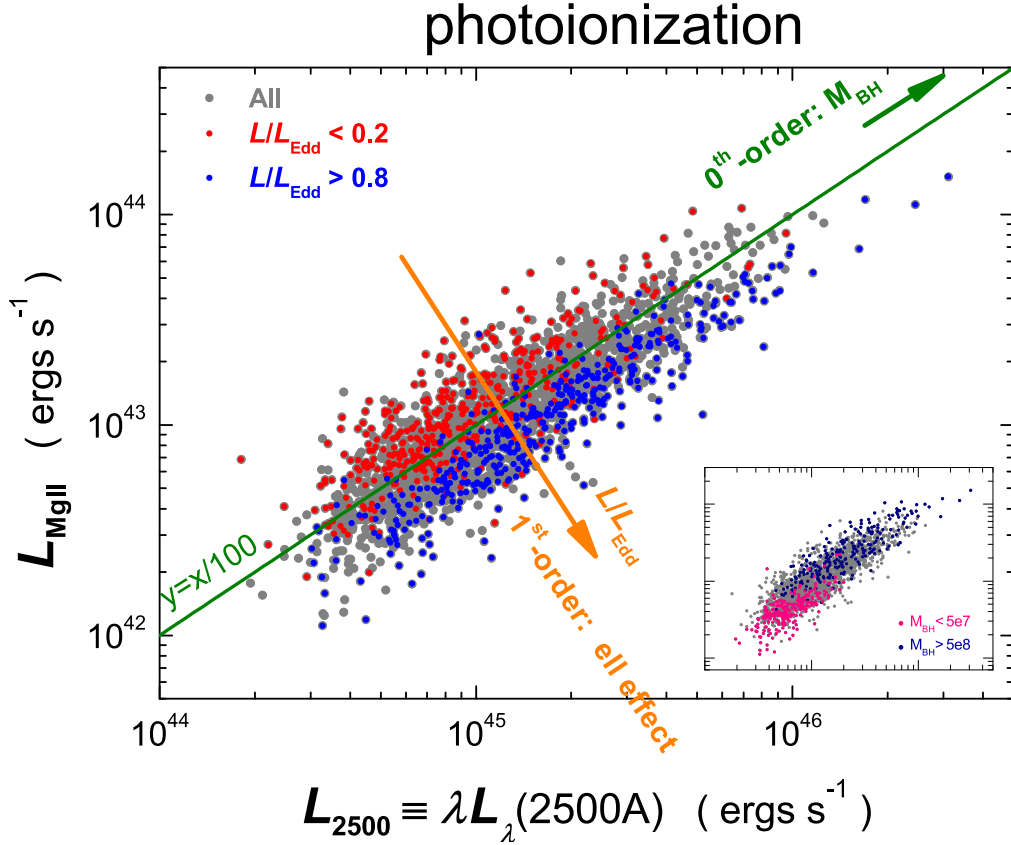


Figure 4. The log-log plot of Mg II versus continuum luminosity relation for the 2092 objects. The green line is the 1-to-100 relation to aid the eye. Inset is the plot of the same data, with objects having $M_{\text{BH}} < 5 \times 10^7 M_{\odot}$ denoted as pink and objects having $M_{\text{BH}} > 5 \times 10^8 M_{\odot}$ navy-blue. Note that $L_{\text{MgII}} = k(\ell) L_{2500} \simeq k_0 L_{2500} \ell^{k'}$. The 0th-order term, k_0 , can be calculated by the classical LOC photoionization of Baldwin et al. (1995); the 1st-order term, $\ell^{k'}$, by the ell effect (cf. Fig. 3c). See Dong et al. (2009b) for details.